Journal of Breath Research

PAPER

Real-time human respiration carbon dioxide measurement device for cardiorespiratory assessment

Om Prakash Singh[1], **Teo Aik Howe**[2] **and MB Malarvili**[1]

[1] Bio-signal Processing Research Group (BSPRG), Faculty of Biosciences and Medical Engineering, Universiti Teknologi Malaysia (UTM), 81310 Skudai, Johor Bahru, Johor, Malaysia
[2] Emergency Department, Hospital Pulau Pinang, Pinang, Malaysia

E-mail: bioom85@yahoo.com

OPEN ACCESS

RECEIVED
31 August 2017

ACCEPTED FOR PUBLICATION
20 September 2017

PUBLISHED
3 January 2018

Keywords: infrared CO_2 sensor, Arduino Mega2560, TFT, cardiorespiratory, reliability, validation, evaluation

Supplementary material for this article is available online

Abstract

The development of a human respiration carbon dioxide (CO_2) measurement device to evaluate cardiorespiratory status inside and outside a hospital setting has proven to be a challenging area of research over the few last decades. Hence, we report a real-time, user operable CO_2 measurement device using an infrared CO_2 sensor (Arduino Mega2560) and a thin film transistor (TFT, 3.5″), incorporated with low pass (cut-off frequency, 10 Hz) and moving average (span, 8) filters. The proposed device measures features such as partial end-tidal carbon dioxide ($EtCO_2$), respiratory rate (RR), inspired carbon dioxide (ICO_2), and a newly proposed feature—Hjorth activity—that annotates data with the date and time from a real-time clock, and is stored onto a secure digital (SD) card. Further, it was tested on 22 healthy subjects and the performance (reliability, validity and relationship) of each feature was established using (1) an intraclass correlation coefficient (ICC), (2) standard error measurement (SEM), (3) smallest detectable difference (SDD), (4) Bland–Altman plot, and (5) Pearson's correlation (r). The SEM, SDD, and ICC values for inter- and intra-rater reliability were less than 5% and more than 0.8, respectively. Further, the Bland–Altman plot demonstrates that mean differences $\pm$ standard deviations for a set limit were 0.30 ± 0.77 mmHg, -0.34 ± 1.41 mmHg and 0.21 ± 0.64 breath per minute (bpm) for CO_2, $EtCO_2$ and RR. The findings revealed that the developed device is highly reliable, providing valid measurements for CO_2, $EtCO_2$, ICO_2 and RR, and can be used in clinical settings for cardiorespiratory assessment. This research also demonstrates that $EtCO_2$ and RR (r, -0.696) are negatively correlated while $EtCO_2$ and activity (r, 0.846) are positively correlated. Thus, simultaneous measurement of these features may possibly assist physicians in understanding the subject's cardiopulmonary status. In future, the proposed device will be tested with asthmatic patients for use as an early screening tool outside a hospital setting.

1. Introduction

Human respiration carbon dioxide (CO_2) contains significant information that can assist physicians in identifying spot ventilation derangements, extubation outcomes, bronchospasm and the effectiveness of therapy in the operating room, neonate intensive care units, intensive care units (ICU), critical care units (CCU) and in the clinical environment [1–3]. Further, features extracted from CO_2 signals, such as $EtCO_2$, respiratory rate (RR), time spent at $EtCO_2$, exhalation duration, Hjorth parameters (activity, mobility and complexity), $V_{CO^2} \times$ slopeIII/RR, end-exhalation slope, the slope ratio (SR), and area ratio can be used to monitor and diagnose cardiopulmonary diseases, such as chronic obstructive pulmonary disease (COPD), asthma, congestive heart failure (CHF), pulmonary embolism (PE), and pneumonia [4–12]. To date, to the best our knowledge, the capnograph is the only device on the market that serves this purpose.

A capnograph is a non-invasive device that uses infrared technology and measures human respiration CO_2 from expired gases and an incessant plot of exhaled CO_2 over time, known as a capnogram. A

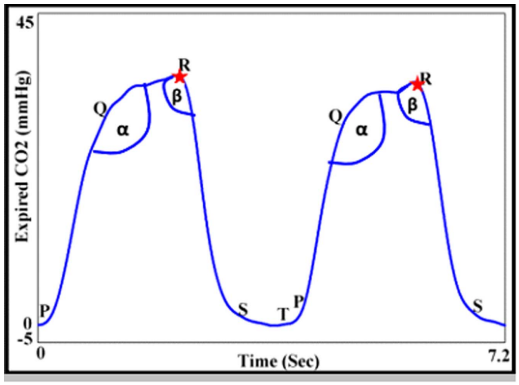

Figure 1. Expiration, alveolar plateau, and inspiration phases of a capnogram signal. P: the onset of expiration; PQ segment: mixture of dead space and alveolar gases; QR segment: plateau phase showing alveolar gas delivery; RL: indicates the end of expiration; RS segment: initiation of inspiration; ST: low CO_2 concentration in the airway during the remainder of inspiration.

capnogram signal looks like a square wave; a complete two-breath cycle from a 2 min recording of a capnogram signal is displayed in figure 1. Each breath cycle has four phases and two angles (see figure 1). 'PQ', 'QR', 'RS', and 'ST' indicate the expiration, alveolar, the beginning of inspiration, and latency phase, respectively, whereas both angles (α and β) represent transitions between PQ, QR, and RS. Further, 'R' signifies the utmost value of CO_2 at the end of the breath that is designated as $EtCO_2$ [13–15].

However, these features have not been incorporated into capnography in a clinical setting as the findings are performed in an offline mode. Besides, capnography is bulky and expensive, and provides a poor estimation of the ventilation and perfusion (V/Q) status of the lung [16]. Therefore, there is an urgent need for a lightweight, inexpensive, precise, and quantitative CO_2 measurement device. Hence, in this paper, we propose a real-time human respiration CO_2 measurement device that can be used for cardiorespiratory assessment in a user friendly environment. In order to develop the proposed device, there are some important points to consider: namely, CO_2 features, existing technology, and a proper CO_2 sensor. These points are discussed in detail in the subsequent sections.

1.1. Significance of CO_2 features

Over the past few decades, many studies have been conducted on the extraction of capnogram features in association with heart–lung diseases [7–12, 17–26]. Of these, the study documented by Yaron *et al* [17] in 1996 investigated a parameter (alveolar slope) and measured the slope (dCO_2/dt) for five consecutive expired breaths among 18 asthmatic subjects. They concluded that the slope of the plateau of the capnogram varies from 0.27 ± 0.05–0.19 ± 0.07 for asthmatic patients during pre- and post medication. Since then, it has become increasingly apparent that the capnogram provides a new way to monitor the inflammatory status in cardiorespiratory disorders. Later, Guthrie *et al* [18] employed a microcap plus device (Oridion Capnograph, Israel) for the measurement of $EtCO_2$ on 16 asthmatic patients, and suggested that non-invasive bedside measurement of $EtCO_2$ is feasible among children suffering from acute asthma. Further, Nagurka *et al* [19] studied the changes in extreme (both low and high) $EtCO_2$ on 299 asthmatic patients and recommended that initial $EtCO_2$ measurements may be a biomarker for asthmatic conditions outside a hospital setting. Further, Kesten *et al* [9] examined the RR correlation between 47 acutely ill asthmatic patients and 42 non-asthmatic patients. They concluded that RR increases during an asthma attack, which coincides with the findings of Kassabian *et al* [20] and Azab *et al* [21]. However, further studies are required to determine the feasibility of $EtCO_2$ and RR for the early detection of asthma episodes beyond a clinical assessment.

In addition, Howe *et al* [22] investigated four features (the α-angle and slope of three different phases of a capnogram) in connection with asthma using Novametrix® capnometry among 30 asthmatic patients. The findings revealed that the slope of the phase III and α-angle can be used as indices to monitor asthmatic conditions. To support these finding, Kean *et al* [11] and Hisamuddin *et al* [23] both advocated considering the slope of the phase III and α-angle as indices for the diagnosis of asthma. In addition, Kean *et al* [11] also introduced new indices (Hjorth parameters, SR, area ratio) to identify asthmatic conditions. They concluded that the SR and the newly introduced Hjorth parameters (HP2—mobility) were the best parameters to discriminate between asthma and non-asthma. Further, Mieloszyk *et al* [10] explored four physiological parameters (exhalation duration, maximum CO_2, time spent at maximum CO_2, and end-exhalation slope) from 30 healthy, 56 COPD, and 53 CHF subjects using a capnogram signal, and correlated their findings with COPD versus CHF and COPD versus normal subjects. The results were statistically significant with a receiver operating characteristic curve of 0.89 for COPD/CHF classification, and 0.98 for COPD/healthy classification. So far, most studies have been carried out offline for the extraction and analysis of the capnogram's features showing a strong correlation with obstructive lung diseases. Hence, the incorporation, implementation, and feasibility of these features while developing a real-time human respiration CO_2 measurement device are yet to be verified. This motivated us to develop a real-time, quantitative human respiration CO_2 measurement device with the disclosed features.

1.2. Available technology for the development of the CO_2 measurement device

The side- and mainstream techniques are used for the development of the CO_2 measurement device as a

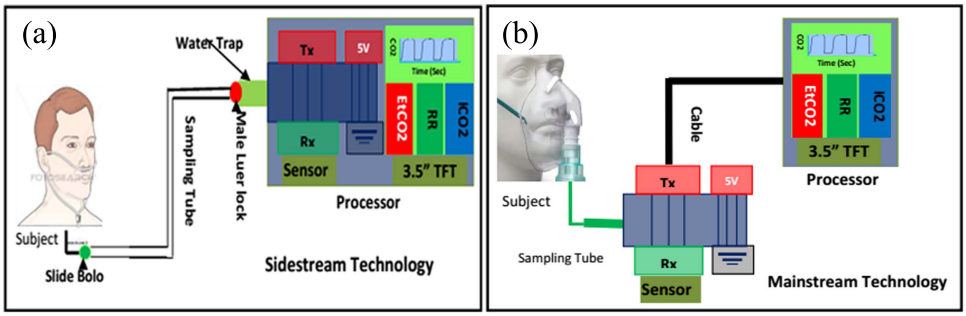

Figure 2. CO_2 measurement technology: (a) sidestream, and (b) mainstream.

function of time or volume, as illustrated in figures 2(a) and (b). In the sidestream technique, a CO_2 sensor is placed inside the main unit, away from the subject, to detect the CO_2 molecules. A mini pump aspirates the sample from the sampling tube at a sampling rate of 50–200 ml min^{-1} which ensures the sidestream capnograph is reliable for both adults and children [10]. Hence, the sidestream technique has been found to be more convenient, simple and easy to sterilize compared with the mainstream technique. In addition, it can be used when a patient is in an unusual position [27, 28].

In contrast to the sidestream technique, a CO_2 sensor is placed between the endotracheal tube and the breathing circuit in the mainstream method. Hence it does not require a sampling tube, pump, motor, and scavenges. In addition, the mainstream capnograph has a faster response time, a simple mechanism and a more accurate sampling rate. However, mainstream CO_2 sensors are relatively expensive, heavy and require solid state sources, improved optics, and miniaturization [29]. Furthermore, the mainstream CO_2 sensor is heated above body temperature, about 40 °C, in order to prevent water vapor condensation, which may burn the patient's skin [29, 30]. Hence, we considered developing a time-based sidestream real-time CO_2 measurement device based on a non-dispersive infrared (NDIR) CO_2 sensor, which is considered to be the predominant form in a hospital setting [10].

1.3. Selection of infrared CO_2 sensor

Over the last few years, many NDIR CO_2 sensors, such as Sprint IR [3, 31], MG811 [32], COZIR [33], COMET [34], and MH410 [35], have been explored for the development of a respiration CO_2 measurement device. Of these, COMET is considered as the most suitable sensor due to its unique specifications (warm-up time, response time, weight, and output), as presented in table 1.

Table 1 illustrates that the warm-up time, response time, weight, and output range of the COMET CO_2 sensor is 2–15 s, 0.028 s, <7 g and 0%–13.8%, respectively. These specifications indicate that the COMET CO_2 sensor is highly selective and sensitive to CO_2 gas compared to other sensors.

Table 1. Comparison of the specifications of various NDIR CO_2 sensors used in the development of a CO_2 measurement device.

CO_2 sensor	Warm-up time (s)	Response time (s)	Weight (g)	Reference
Sprint IR	<60	0.05	8	[3, 31]
MG811	300	<60	60	[32]
COZIR	<10	4–120	20	[33]
COMET	2–15	0.028	<7.0	[34]
MH410	90	<30	20	[35]

s = second.

In addition, the sampling rate (100 samples per s) of the COMET is comparatively high and provides more precise and detailed analysis of the CO_2 signal. Hence, our developed CO_2 measurement device uses an NDIR CO_2 sensor equivalent to COMET [36] to acquire the CO_2 signal. The NDIR sensor absorbs the CO_2 molecules at a specific wavelength (4.3 μm) in the infrared region and follows Beer–Lambert law, as given in equation (1) [37–39]. This avoids any recompense when different concentrations of N_2O, O_2, anesthetic agents, and water vapor are present in the inspired and expired breath:

$$I = I_0 e^{-\alpha b t} \quad (1)$$

where I represents the intensity of the light hit on the detector (W cm^{-2}), I_0 is the considered intensity of the empty chamber (W cm^{-2}), α is the absorption coefficient (cm^2 mol^{-1}), b is the concentration of CO_2 (cm^2 mol^{-1}), and t is the length of the absorption path (cm).

Thus, for the first time, we report a real-time, and highly reliable human respiration CO_2 measurement device with the incorporation of a first order low-pass filter with a cut-off frequency (fc = 10 Hz) and a moving average filter (span, 8). In this paper, the complete research work is organized as follows. In section 2, we explain the technical details of the components used in our research study, followed by the computation and transmission processing algorithm, which includes feature extraction, the noise reduction method, and CO_2 data display as presented in the supplementary information (available online at stacks.iop.org/JBR/12/026003/mmedia). In section 3, we report the data

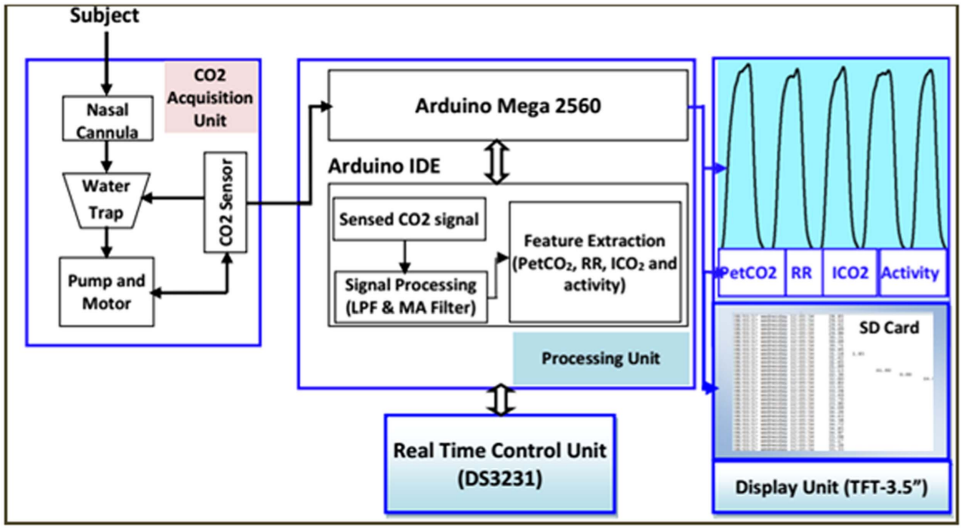

Figure 3. Block diagram of the respiration CO_2 measurement device; CO_2 acquisition unit (nasal cannula, water trap, pump, motor and NDIR CO_2 sensor), processing unit (AtMega2560 and arduino IDE), display unit (3.5″), displays (CO_2 signal, Hjorth parameter, $EtCO_2$, ICO_2 and RR), real-time control unit, and secure digital card (8 GB).

collection and recording procedures along with the statistical method used for the performance (reliability and relationship) evaluation of the device. In section 4, we present our results, followed by a discussion of the significance of the retrieved features, signal processing techniques, and performance of the developed device in section 5. Finally, in section 6, we conclude and outline the directions for future research in this area.

2. Material and methods

2.1. Overview of the human respiration CO_2 measurement device

Figure 3 shows a block diagram of the CO_2 measurement device. The device is comprised of four parts, namely a CO_2 acquisition unit, processing unit, real-time control (RTC) and a display unit. The CO_2 signal is acquired from the subjects through a sampling tube and is passed to a microcontroller unit for computation and transmission purposes. Further, the CO_2 signal and other parameters ($EtCO_2$, RR, ICO_2, and activity) are extracted and displayed on a thin film transistor (TFT) through serial communication. With this, $EtCO_2$ reflects the maximum CO_2 concentration of alveoli emptying last, RR is the rate at which breathing occurs, ICO_2 represents the amount of CO_2 concentration inhalation during breathing that provides information regarding the rebreathing of CO_2 which is caused due to an improper breathing circuit setup or a patient's unusual conditions, and activity is the first Hjorth's parameter that measures the mean power of each breath signal. The analysis considered the slopes of the curve, which shows a strong correlation with the CO_2 signal. The calculation of the activity is based on variance, hence the computational cost of this method is low compared to other methods. In addition, data logging on an SD card is performed through an RTC which is controlled by a processing unit. The technical details of the components are explained in the supplementary information. In addition, the feature extraction and display processes of the CO_2 signal are presented in the supplementary information. Thereafter, the device performance is evaluated using statistical methods.

3. Performance evaluation of the proposed device

3.1. Data collection and recording procedures

In this study, a total of 22 healthy participants aged between 21 and 35, (12 females, 23.85 $\pm$ 4.02; 10 males, 29.81 $\pm$ 3.75) were recruited from the Faculty of Biosciences and Medical Engineering, Universiti Teknologi Malaysia (UTM) using random sampling [40], and the characteristic details of the participants are presented in table 2. An informed consent was obtained from all the participants before participating in the study. The data are presented in mean $\pm$ SD unless otherwise specified.

All the participants were asked to sit comfortably in a chair with a backrest for 10 min and advised not to participate in strong physical activity to avoid any alteration in the $EtCO_2$, RR and activity values, as presented in figures 4(a) and 5(b), respectively. Then, the participants were instructed to breathe in and out through the nasal cannula in a normal, relaxed manner at their own pace. All the data ($EtCO_2$, RR, ICO_2 and activity) were recorded simultaneously for 2 min [41]. To check the reliability and validity of the developed device further, statistical methods were used.

Table 2. Characteristic details of healthy subjects ($n = 22$) presented by age and gender.

		Age (Y)		Weight (Kg)		Height (m)		BMI (Kg m^{-2})	
Age	Gender (n)	X	SD	X	SD	X	SD	X	SD
20–29	M (4)	25.75	2.75	72.75	9.91	1.68	0.03	25.67	3.20
	F (12)	22.58	1.97	55.89	8.93	1.56	0.06	22.87	3.26
30–35	M (5)	31.80	2.48	76.00	16.83	1.72	0.07	25.56	5.37
	F (1)	30.00	0.00	75.00	0.00	1.5	0.00	33.33	0.00

F = female, M = male, X = mean, SD = standard deviation, BMI = body mass index, Y = years, m = meter.

Figure 4. The subjects' posture during the experiment: (a) (F, age 22), and (b) (M, age 30). The nasal cannula was attached into the nose to acquire and transport the CO_2 signal through the sampling tube (length: 7 feet).

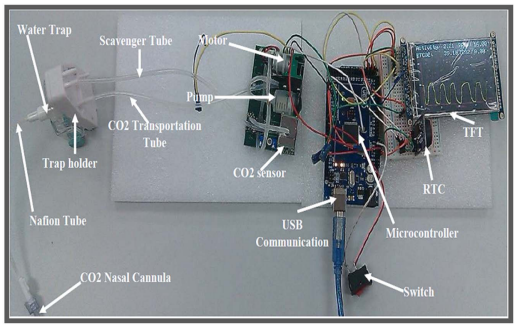

Figure 5. Complete set-up of the device (preliminary model), assembled with a few components, such as a nasal cannula, water trap, nafion tube, CO_2 sensor, motor, pump, Arduino Mega2560, switch, RTC module and display (TFT, 3.5″).

3.2. Statistical method for performance (reliability and validity) analysis

A repeated measures design was adopted to examine the inter- and intra-rater reliability of the device for a CO_2 signal, $EtCO_2$, RR, and activity. The reliability studies were carried out by certified researchers of the Good Clinical Practice on different occasions in compliance with the UTM Health Center's ethical clearance standard. Reliability analysis helps to confirm whether the output is consistent or not when the test is performed by the same or different users with dissimilar times. In addition, it is believed that a device cannot be valid until it is reliable [42]. Hence, in this study, we have examined both the reliability and validity of the newly developed device. To test the validity, data were recorded using a standard capnograph device (CapnostreamTM[20] Model CS08798) and the developed respiration CO_2 measurement device for each subject for 2 min.

For this, descriptive statistics (mean and standard deviation) of the CO_2 signal, $EtCO_2$, RR, and Hjorth's parameter (activity) were calculated for all participants, both male and female. Further, the normality distribution of each feature was analyzed with respect to each measurement. For this, the skewness and kurtosis, z-values and Shapiro–Wilk p-values were calculated for a dependent variable to verify the normality of the data for both males and females. The z-value ($-1.96 <= z <= 1.96$) and Shapiro–Wilk p-value ($p > 0.05$) were considered statistically significant [43–47].

Further, the intraclass correlation coefficient (ICC) and its 95% confidence interval (CI) were used to quantify the inter- and intra-rater reliability. In addition, to verify the level of absolute reliability and sensitivity, SEM and SDD were calculated using equations (2) and (3), respectively [48, 49]. The convention of Rosner was adopted to describe the strength of the ICCs (ICC < 0.40 = poor reliability; $0.40 \leqslant$ ICC < 0.75 = fair to good reliability, and ICC $\geqslant 0.75$ = excellent reliability) [50, 51]. Further, the outputs of both devices were compared using Bland–Altman analysis and the acceptable limit was set at $\pm 10\%$ for CO_2, $EtCO_2$, and RR values, respectively [52]. Additionally, the Pearson correlation coefficient was calculated to determine the relationship between the features. Statistical analysis was performed using SPSS (SPSS 23.0 for Windows) and the significance was set at $p < 0.05$. The results are presented in section 4:

$$\text{SEM} = \text{SD} \times (\sqrt{1} - \text{ICC}), \quad (2)$$

$$\text{SDD} = 1.96 \times \sqrt{2} \times \text{SEM}, \quad (3)$$

where, SD is the standard deviation and ICC represents the intraclass correlation coefficient value.

4. Result

4.1. Real-time human respiration CO_2 measurement device

We report a real-time quantitative and user-operable human respiration CO_2 measurement device based on

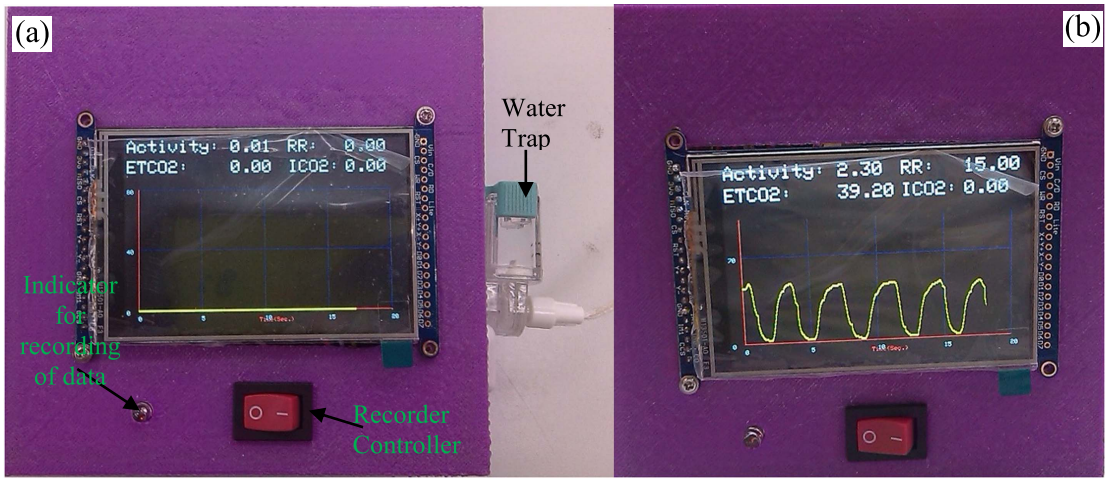

Figure 6. (a) The ideal, and (b) active state of display of the CO_2 signal and associated features. (A video for this figure is available online at stacks.iop.org/JBR/12/026003/mmedia.)

sidestream technology that can be used inside and outside a hospital setting. In addition, LPF (fc, 10) and MAF (span, 8) were employed in order to reduce noise and to provide a smooth CO_2 signal. This helped in extracting specific and precise features from the CO_2 signal. A preliminary model (the internal arrangement of components) of the device is presented in figure 5.

In this preliminary study, we preferred to extract $EtCO_2$, RR, ICO_2, and the Hjorth parameter (activity) due to the unfussiness and ease of implementation of the algorithm (see the supplementary information) and displayed all the parameters onto the TFT along with the CO_2 signal. These parameters ($EtCO_2$, RR, and ICO_2) were exhibited for each breath whereas Hjorth's parameter (activity) was measured for every breath and the mean of two consecutive breaths was displayed. With this, $EtCO_2$ reveals the maximum amount of CO_2 which exits the alveolus and increases during a blockage in the air track when the subjects do not adequately eject CO_2 during expiration, RR displays the breathing pattern that may increase or decrease depending on the subject's severity of gasping efficiency, and ICO_2 reveals the rebreathing of CO_2 gas. Figures 6(a) and (b) indicate the ideal and active state, respectively, of the display where the horizontal axis denotes the time, ranging from 0–20 s, and the vertical axis indicates expired CO_2, ranging from 0–80 mmHg.

Figure 6(a) shows the retrieved features and the CO_2 signal to be zero ('0'), as the nasal cannula was not subjected to testing. Figure 6(b) shows the CO_2 signal and associated features for a healthy subject (e.g. $EtCO_2$, 39.20 mmHg; RR, 15 bpm; ICO_2, 0.00 and activity, 2.30) as soon as the sample line is fastened. There was a sweep in the CO_2 signal after 19.98 s due to a loss of 0.02 s when starting from the beginning. Additionally, the obtained parameters and CO_2 signal were saved onto an SD card (8 GB) through an RTC unit (DS3231), as presented in figure 7. With this, each data point was saved inside a folder with respect to date, day, and time with a delay of 10 ms, providing an easy method of accessing the subject's information in the future. The code for each folder has a designated ID containing the current date. In this, the saving procedure was controlled by a mechanical switch that saves the data. With every press, a new file was generated according to the hour, minute, and second of the day, depending upon the need of the subject or observer. Further, we have discussed the performance of the filter and device in subsequent sections.

4.2. Implementation of filters

A 10 Hz FIR low-pass filter was applied to limit the bandwidth and remove the upper-frequency components of the CO_2 signal. Figure 8(a) shows raw (red dash line) and filtered (blue dot point) CO_2 signals. This clearly shows that CO_2 signals fall within 10 Hz. A further moving average filter (span, 8) was applied to provide smooth CO_2 signals in order to avoid any imprecision while extracting the features. In addition, it also removed random noise while preserving the sharp step response, making it the foremost, optimal filter for a time domain programmed signal. Figure 8(b) shows the raw (red line) and smoothed CO_2 signal (blue line) for five consecutive breaths, extracted from a 2 min recorded signal. The raw CO_2 signal seems to be noisy, disturbed and has an irregular shape that may provide an inaccurate result, whereas the filtered signal appears very smooth and crisp, with regular shapes and a resolution of more than 99.10% of the raw CO_2 signal.

In addition, the correlation coefficient was calculated for each CO_2 signal after filtering (low pass and moving average) for a justified cut-off frequency and span width, respectively. For example, the correlation coefficient for one of the subject's signals after a low

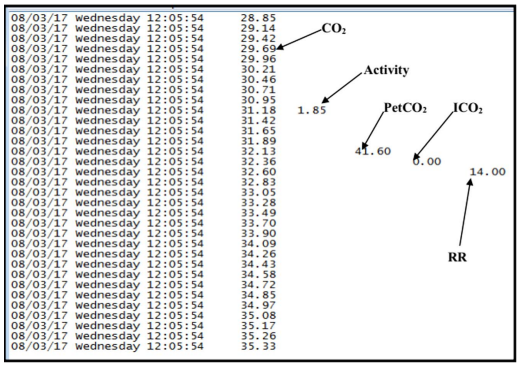

Figure 7. Data (CO_2, activity, $EtCO_2$, ICO_2, RR) logging with date, day, and time.

pass and moving average filter was 1.000 and 0.9910672, respectively.

4.3. Performance evaluation (reliability and validity)

Further, the developed device was tested on 22 healthy subjects, in order to ascertain the reliability, validity and relationship of each feature. The recording procedures have been explicated in section 3. The result revealed that the mean and SD values of $EtCO_2$, RR and activity were 39.57 ± 2.91 mmHg, 17.00 ± 2.33 bpm, and 1.69 ± 0.45, respectively, whereas the ICO_2 was 0.00 mmHg for all the healthy subjects, as presented in figure 9. Further, the normality distribution of the data was verified using skewness and kurtosis, *z*-values and Shapiro–Wilk *p*-values. Our findings demonstrate that each feature shows little skewness and kurtosis for both males and females, but it does not differ significantly from normality. Hence, we assume that our data are approximately normally distributed in terms of skewness and kurtosis. Besides, Shapiro–Wilk *p*-values are found above 0.05 for each feature for both males and females. Therefore, we maintained a null hypothesis, and in terms of the Shapiro–Wilk test, we assume that data are approximately normally distributed. Thus, the inter- and intra-rater reliability test was assessed based on ICC, SEM and SDD, and the validity was assessed using Bland–Altman plot analysis, whereas a relationship was established using Pearson correlation coefficients (*r*).

4.3.1. Reliability analysis

The inter- and intra-rater reliability test was conducted on two dissimilar occasions by two observers. The ICC values (95% CI), SEM and SDD of inter- and intra-rater reliability for all the parameters are summarized in tables 3 and 4, respectively.

In our study, for inter-rater reliability, the ICC ranged from 0.88–0.96 with an average (95% CI 0.83–0.97); SEM and SDD values ranged from 0.23–1.80 and 0.65–4.99, respectively. For intra-rater reliability, the obtained ICC ranged from 0.78–0.96 with an average (95% CI 0.72–0.95); SEM and SDD values ranged from 0.38–1.58 and 1.07–4.39, respectively. The obtained ICC values for both reliabilities were greater than 0.8, except the activity (intra-rater ICC, 0.783) which revealed that the developed device is highly reliable for all the measured parameters. In addition, the SDD and SEM values were found to be lower than 5% for all the measured parameters, revealing the high level of absolute reliability and sensitivity, i.e. measurement error was low and accuracy was high. Therefore, one or more observers can use the device and its features for the measurement of a CO_2 signal with little variation, demonstrating the device's ease of use.

4.3.2. Validation of the device and its features

The precision of the device was verified using a Bland–Altman plot by comparing data obtained from the developed device and standard capnography (CapnostreamTM[20] model CS08798). Figures 10(a) and (b), 11(a) and (b) and 12(a) and (b) show Bland–Altman plots, generated for CO_2, $EtCO_2$, and RR measurements respectively. The plots display a data point for each subject, where the *x*-coordinate is the average of the two device measurements and the *y*-coordinate is the difference between the measurements as a percentage of the average. The 95% limit of agreement between the mean differences for CO_2, $EtCO_2$ and RR from standard capnography and the readings from our device were 1.8 mmHg and −1.2 mmHg (9.03% and −6.09%), 2.42 mmHg and −3.10 mmHg (6.24% and −7.99%) and 1.47 bpm and −1.04 bpm (8.51% and −5.94%), respectively. It also revealed that the mean differences from the actual values are closer to zero with bias inaccuracy for CO_2, $EtCO_2$, and RR, which were 0.30 mmHg (1.47%), −0.34 mmHg (−0.87%) and 0.21 bpm (1.28%), respectively. Thus, the robustness of the developed device in measuring different parameter values (CO_2, $EtCO_2$ and RR) with the same performance is guaranteed compared with standard capnography.

4.3.3. Relationship between $EtCO_2$, RR, and activity

The reason for establishing this relationship is that the study conducted by Kesten *et al* [9], Nagurka *et al* [19], Kassabian *et al* [20], Azab *et al* [21], Guthrie *et al* [18], Brown *et al* [7] and Kean *et al* [11], reported that during asthmatic and CHF attacks, RR increases whereas $EtCO_2$ and Hjorth's parameter (activity) decreases. However, to the best of our knowledge, to date, no study has been performed combining all these parameters in correlation with cardiorespiratory conditions due to a lack of evidence. Hence, to verify the findings, we performed bivariate correlation analysis between these parameters to assess the relationship between $EtCO_2$, RR, and activity. The relationship between $EtCO_2$, RR, and activity is shown in figures 13(a), (b). Figure 13(a) shows that $EtCO_2$ and RR ($r = -0.70$, $N = 22$ and $p = 0.000$) are negatively

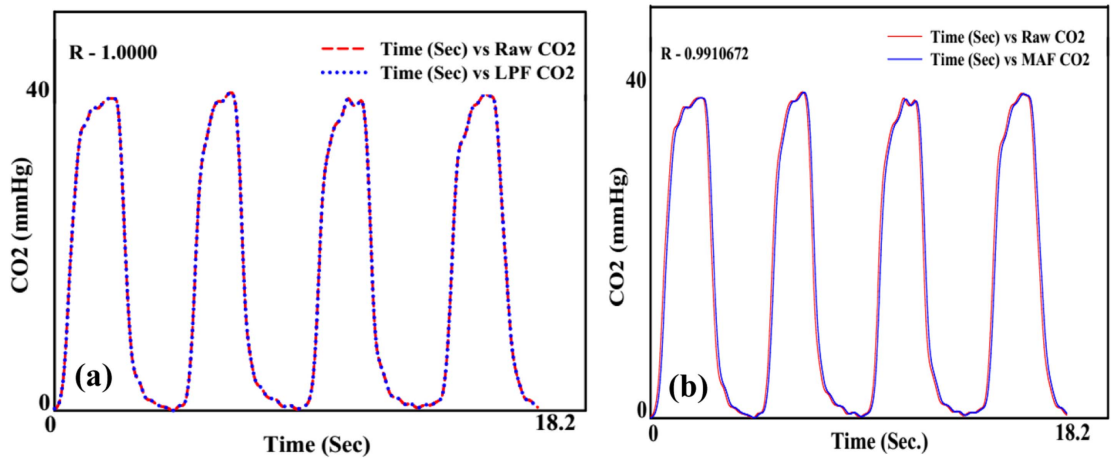

Figure 8. (a) Original CO_2 signal (red dash line) and low-pass filtered (fc, 10 Hz) CO_2 signal (blue dotted line), and (b) raw and moving average filtered (smoothed) CO_2 signal of a healthy subject.

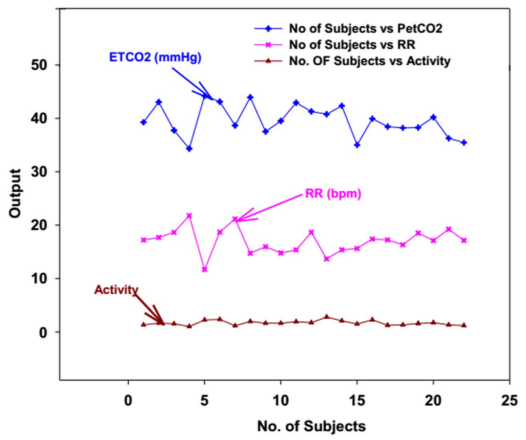

Figure 9. Normality value of $PetCO_2$, RR, and activity of healthy subjects.

Table 4. The standard error of measurement (SEM) is stated in millimeters of mercury (mmHg) and breath per minute (bpm), respectively for $PeCO_2$, $EtCO_2$, and RR. The small detectable difference (SDD) is dimensionless.

SEM and SDD ($n = 22$), respiration CO_2 measurement device			
Features	Rater	SEM	SDD
$PeCO_2$	Inter-rater	1.08	3.00
	Intra-rater	1.42	3.94
$EtCO_2$	Inter-rater	1.80	4.99
	Intra-rater	1.58	4.39
RR	Inter-rater	1.49	4.13
	Intra-rater	1.54	4.28
Activity	Inter-rater	0.23	0.65
	Intra-rater	0.38	1.07

Table 3. Features extracted from the CO_2 signal for a 2 min recording and reliability test ($n = 22$).

Features	Inter-rater, ICC (95% CI)	Intra-rater, ICC (95% CI)
$PeCO_2$	0.957 (0.895–0.982)	0.920 (0.809–0.967)
$EtCO_2$	0.963 (0.909–0.985)	0.968 (0.924–0.987)
RR	0.888 (0.732–0.953)	0.862 (0.673–0.942)
Activity	0.922 (0.810–0.968)	0.783 (0.484–0.909)

$PeCO_2$ = exhaled carbon dioxide; $EtCO_2$ = partial end-tidal carbon dioxide; RR = respiratory rate; CI = confidence interval; ICC = intraclass correlation coefficient; n = number of healthy subjects.

correlated. The figure shows a simple scatter regression graph which reveals that as $EtCO_2$ increases, RR tends to decrease, and the data points are in line with the regression line, revealing that both have a moderately strong linear association. Figure 13(b) shows that $EtCO_2$ and activity ($r = 0.85$, $N = 22$ and $p = 0.000$) are positively correlated. $EtCO_2$ and activity both increase simultaneously. Additionally, the values of $EtCO_2$ and activity are very near the line, specifying a strong linear relationship. Thus, the finding reveals that there is a moderately strong relationship between EtCO2, RR, and activity. Hence a concurrent measurement of these parameters may possibly help health care professionals to evaluate the patient's cardiopulmonary status.

5. Discussion

To date, no studies have reported the incorporation of both a noise reduction algorithm and newly introduced features in correlation with cardiopulmonary assessment in real time. An earlier study presented a sidestream capnograph which measured $EtCO_2$, RR and a capnogram. However, the device was complex and the computation cost was high due to the microcontroller (AtMega 8535) and display (128 × 64), as the data could not be saved [29]. Our developed device measures the features $EtCO_2$, RR, CO_2 and the newly introduced feature, activity, and is displayed on a high resolution TFT (320 × 480). Additionally, it can save the data onto

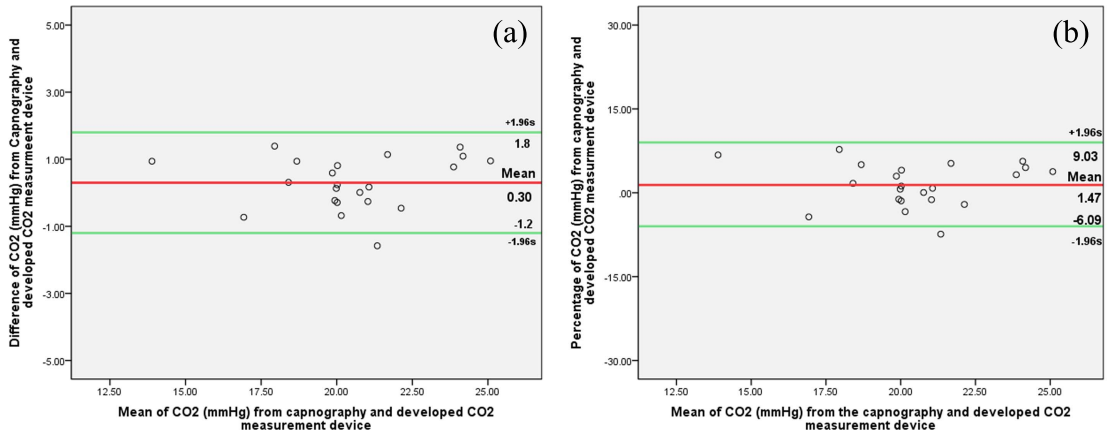

Figure 10. Bland–Altman plots between mean and difference from standard capnogrpahy versus measured CO_2 (a) in mmHg and (b) in percentages. Dashed lines indicate the upper and lower 95% limits of agreement.

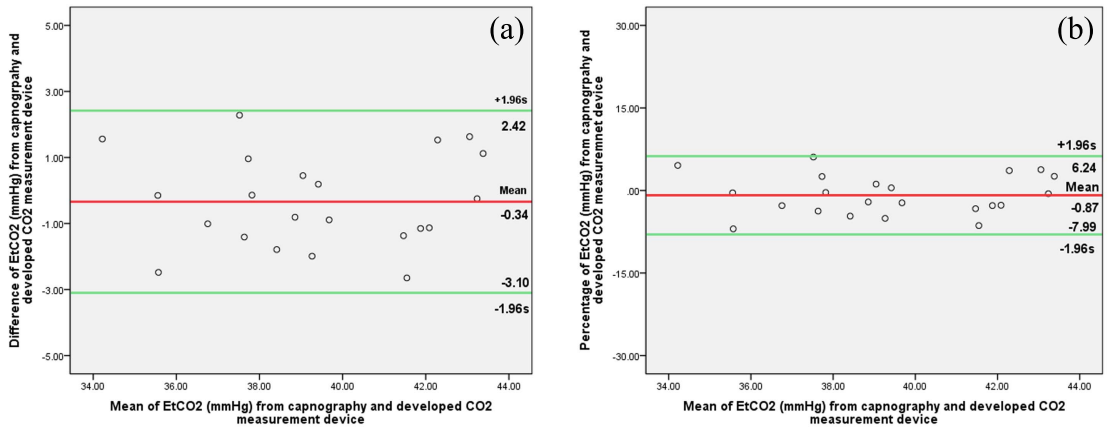

Figure 11. Bland–Altman plots between the mean and difference from standard capnography versus measured $EtCO_2$ (a) in mmHg and (b) in percentages. Dashed lines indicate the upper and lower 95% limits of agreement.

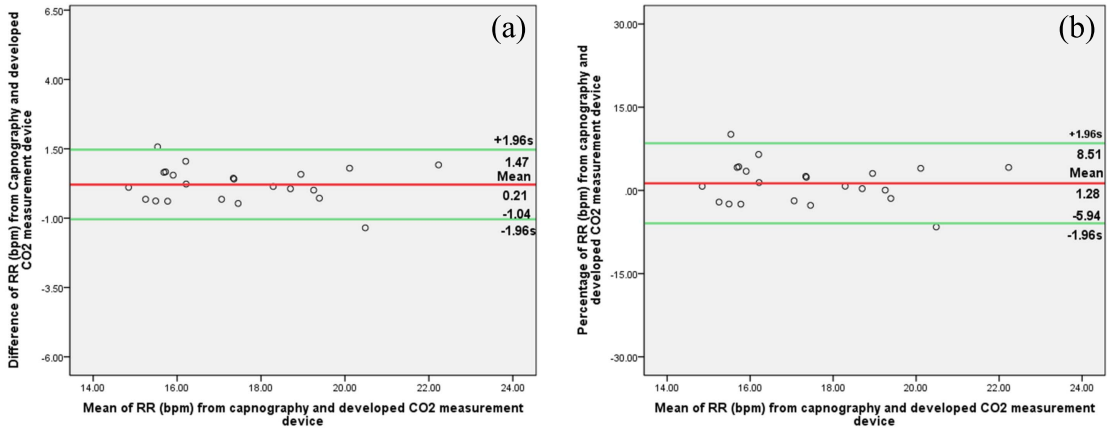

Figure 12. Bland–Altman plots between mean and difference from standard capnography versus measured RR (a) in bpm and (b) in per cent. Dashed lines indicate the upper and lower with 95% limits of agreement.

an SD card via RTC which is mounted with a TFT. We extracted these features in agreement with earlier studies [9–11, 18–21, 53], since these can be used as indices when evaluating the cardiorespiratory condition at a preliminary or extreme level. The research conducted by Kesten *et al* [9], Azab *et al* [21], Guthrie *et al* [18], Nagurka *et al* [19], Kean *et al* [11], Langhan *et al* [53], and Lamba *et al* [8] suggested that the

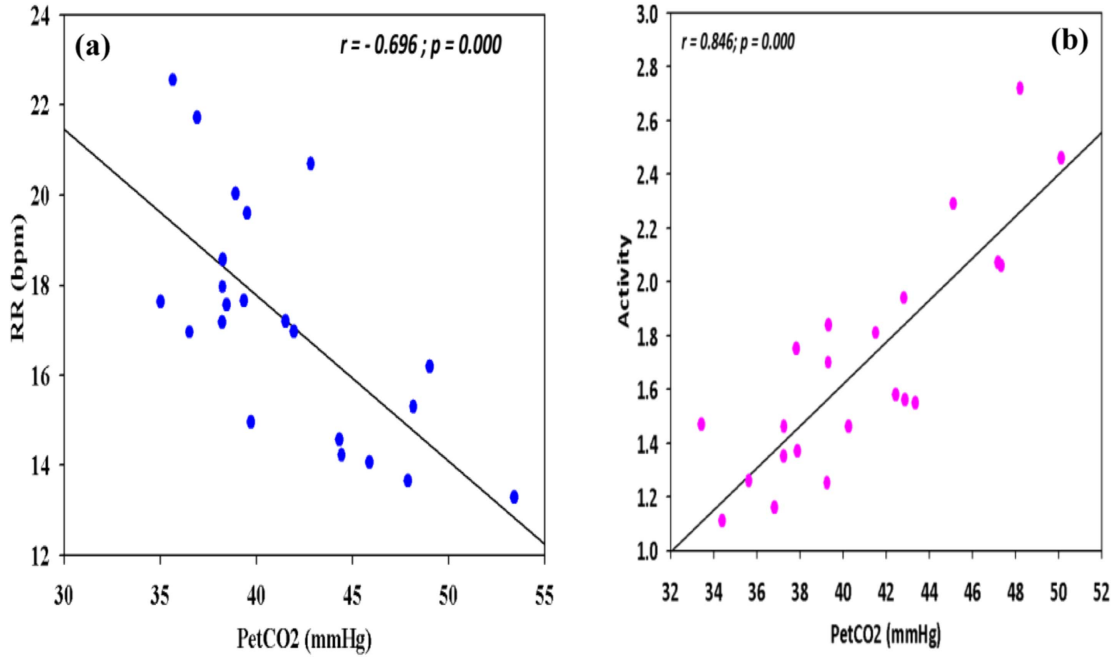

Figure 13. Relationships: (a) EtCO2 versus RR, and (b) EtCO2 versus activity.

measurement of these parameters can help observers to evaluate the obstruction level in the air passage of patients. Kean *et al* also reported that the computation of a new feature (activity) for one breath is capable of discriminating asthmatic and non-asthmatic conditions with an AUC (0.8951) and *p*-value (<0.0001). Further we verified the normality range of each feature based on earlier studies, and findings revealed that the data were in the normal range [53, 54].

Further, a noise reduction algorithm (LPF and MAF) was implemented in real time in order to smooth the shape of the CO_2 signal, helping to extract precise features. LPF was applied in agreement with an earlier study to limit the bandwidth of the signal [55]. The application of two earlier advised 13-span filters for MAF [10, 25, 56] to smooth the signal was tested, and a loss of data of more than 4.9% was found. Hence in our study we apply an optimum span 8 for high resolution (99.1%) compared with previous studies. Further, the consistency of each feature was verified based on relative and absolute reliability analysis [48, 57].

The relative reliability indicates the amount of any changes in the measurement of healthy subjects in each feature measurement, and clarifies, by actual differences, the true value of the attribute being quantified. We found that the ICC value for the inter-rater test was 0.88–0.96; this demonstrates that 88%–96% of the quantity deviation was due to inconsistency in the true value of the measured attribute and 12%–4% to random inter-subject variability. For the intra-rate test, ICC was 0.78–0.96; this demonstrates that the 78%–96% measurement difference was owing to the changeability in the true value of the measured characteristic, and 22%–4% to chance in the intra-subject variability. Since ICC values of more than 0.7% are acceptable in clinical settings, the developed device may provide useful information for diagnostic and classification purposes in cardiopulmonary patients.

In the absolute analysis, the SEM provides an approximation of the error size of each feature and indicates the absolute reliability [48], whereas SDD reveals the sensitivity of the changes in the measured value [48]. Both the SEM and SDD values collectively disclose a change in the index, reflecting the reliability of the indicators [58]. The lower SEM and SDD demonstrate the greater reliability in the accuracy and precision of the measured values. Further, when the SEM value is less than 10% of the average measured or the highest measured score, the quantify error is small, and thus the measurement is reliable [58]. We found that SEM and SDD activity was 0.38% and 1.07% respectively for the intra-rater test, but 0.23% and 0.65% for the inter-rater test compared with other features with less than 5%. Thus, the findings reveal that 68% of the repeat measurements are likely to fall within +1.80 (maximum, SEM) of the true value for each parameter, in agreement with earlier studies [59, 60]. Further, the precision of the developed device is discussed by comparing the output with standard capnography (CapnostreamTM[20] Model CS08798) from Oridion.

From figures 10(a) and (b), 11(a) and (b) and 12(a) and (b), it can be seen that some outliers are observed in the CO_2 and $EtCO_2$ measurements; however, most of the data points fall within the limits of agreement. In addition, SD values were found close to each other with an average value of approximately 5%.

Accordingly, the difference between the measurements of the device for any subject is supposed to be ±10% relative to the bias. Thus, these results show that the differences between both devices measurements are within an acceptable range. Hence, the Bland–Altman plots reveal a reasonable consistency between the measurements of the developed and existing capnography device. Thus, the developed device is capable of providing valid and robust measurements. Hence, it is considered to be a valid monitoring device that can be used as an alternative to a standard capnography device for clinical and home monitoring purposes. Further, a relationship was established using Pearson's coefficient as a proof of hypothesis regarding the correlation between $EtCO_2$, RR and activity during obstructive lung diseases [9, 61].

We found that $EtCO_2$ and RR are negatively correlated with ($r = -0.7$); this reveals that there is a 70% chance of an increase in the RR value during the initial stage of a blockage in the wind pipe, and $EtCO_2$ values decrease, which concurs with the statement from Kesten *et al* [9], and English [61]. Additionally, EtCO2 and activity are positively correlated with ($r = 0.85$) each other and have an 85% probability of an increase in activity with an increase in $EtCO_2$ values. Hence concurrent measurement of these parameters possibly may help health care professionals to evaluate the patient's cardiopulmonary status. In the next section, the strengths and limitations of the device are discussed.

5.1. Device strengths and limitations

The developed device is small in size (12.50 cm × 13 cm × 8 cm), light weight (650 g) and user operable. Hence it can be used by health care professionals in their work place setting, as well as in emergency settings, unlike traditional capnography, in order to evaluate the cardiorespiratory condition. Further, it can be used by individuals who have been affected by cardiorespiratory disorders in their home or work place, and data can be recorded and sent to health professionals via a simple mail transfer protocol. Further, it does not require any special skills or training in order to operate the device, in contrast to existing devices.

In addition, the developed device is incorporated with a noise reduction algorithm that eliminates random noise while preserving the sharp step response during CO_2 data recording, unlike existing devices. Another novel feature of the device is that it estimates Hjorth's parameter (activity) from each breath cycle considering the slope of the CO_2 signal; hence it may be useful for providing obstructive lung disease information, in contrast to existing capnography. In addition, capnography is not only used in ICU to confirm endotracheal intubation, assessment of cardiac output, and the detection of gastric tubes inadvertently placed in the trachea, but it can also be used to identify and assess obstructive lung diseases such as COPD, asthma, and CHF because of changes in the characteristics of the CO_2 waveform. Further, existing capnography devices only measure the maximum and minimum amount of CO_2 and RR from each breath cycle, which does not involve an analysis of the slope of the resultant CO_2 signal and is unable to provide clear information about the ventilation and perfusion status of the lung. Hence, the incorporation of these features are an added advantage that may be useful in recognizing and assessing cardiorespiratory status more efficiently compared with existing devices. On the other hand, the developed device has limitations which warrant caution. The device only saves the measured features (CO_2, $EtCO_2$, RR, ICO_2, and activity) but cannot transfer data to remotely located physicians providing care to a patient either in hospital or elsewhere. Finally, the atmosphere pressure and temperature values should be set as per the location in the sketch to avoid false respiration CO_2 readings while using the sensor.

6. Conclusion and future work

We developed a non-invasive, highly reliable, precise, and user operable real-time human respiration CO_2 measurement device based on sidestream technology that measures expired CO_2. The developed device displays the quantified features such as $EtCO_2$, RR, ICO_2, activity, and CO_2 signal on a small and single screen (TFT), hence minimizing the size of the device. In addition, this is the first device which has been incorporated with low-pass (fc, 10 Hz) and moving average filters (span, 8) after signal conversion (analog-to-digital) that reduces the total computation cost and provides a sharp and smooth CO_2 signal. The developed device has been tested successfully on 22 subjects in order to ascertain the reliability, validity and relationship of the features. The findings revealed that the inter- and intra-rater mean of each parameter was more than 0.75 and mean differences ± standard deviations for a set limit were 0.30 ± 0.77 mmHg, −0.34 ± 1.41 mmHg and 0.21 ± 0.64 bpm for CO_2, $EtCO_2$ and RR, which demonstrate that the developed device can be used in a clinical setting. The developed device also enabled frequent measurements of the features over a continuous period of time, and delivered accurate and reproducible readings that are not limited by inter- or intra-observer variability. We also found that the features are strongly correlated, and concurrent measurements may assist the physician in assessing cardiopulmonary conditions. In the future, a performance evaluation of the developed device will be carried out on asthma patients.

Acknowledgments

This research is supported by the Ministry of Higher Education under the prototype research grant scheme (PRGS), vote no. R.J130000.7845.4L669. The authors would also like to express their deepest gratitude to the Universiti Teknologi Malaysia for providing facilities and laboratory equipment. Special thanks to Madhanagopal Jagannathan for his assistance in editing.

Disclosures

The authors declare no conflict of interest.

References

[1] Carmen C, Rasera P M, Gewehr and Domingues A M T 2015 PETCO2 measurement and feature extraction of capnogram signals for extubation outcomes from mechanical ventilation *Physiol. Meas.* **36** 231–42
[2] Jaffe M B and Orr J A 2010 Continuous monitoring of respiratory flow and CO2 *IEEE Eng. Med. Biol. Mag.* **29** 44–52
[3] Malik S A, Singh O P, Nurifhan A and Malarvili M B 2016 Portable respiratory CO_2 monitoring device for early screening of asthma *Proc. ACEC* pp 90–4
[4] Brown R H, Brooker A, Wise R A, Reynolds C, Loccioni C, Russo A and Risby T H 2013 Forced expiratory capnography and chronic obstructive pulmonary disease (COPD) *J. Breath Res.* **7** 017108
[5] Fabius T M, Eijsvogel M M, van der Lee I, Brusse-Keizer M G J and de Jongh F H 2016 Volumetric capnography in the exclusion of pulmonary embolism at the emergency department: a pilot study *J. Breath Res.* **10** 046016
[6] Maestri R, Bruschi C, Olmetti F, Rovere M T L and Pinna G D 2013 Assessment of the peripheral ventilatory response to CO2 in heart failure patients: reliability of the single-breath test *Physiol. Meas.* **34** 1123–32
[7] Brown L H, Gough J E and Seim R H 1998 Can quantitative capnometry differentiate between cardiac and obstructive causes of respiratory distress? *Chest* **113** 323–6
[8] Lamba S *et al* 2009 Initial out-of-hospital end-tidal carbon dioxide measurements in adult asthmatic patients *Ann. Emerg. Med.* **54** S51
[9] Kesten S *et al* 1990 Respiratory rate during acute asthma *Chest* **97** 58–62
[10] Mieloszyk R J *et al* 2014 Automated quantitative analysis of capnogram shape for COPD–normal and COPD–CHF classification *IEEE Trans. Biomed. Eng.* **61** 2882–90
[11] Kean T T and Malarvili M B 2009 Analysis of capnograph for asthmatic patient *IEEE Int. Conf. on Signal and Image Processing Applications* pp 464–7
[12] Baruch K 2008 Advances in the use of capnograph for non-intubated patients *ISRJEM* **8** 3–15
[13] Domingo C, Blanch L, Murias G and Luján M 2010 State-of-the-art sensor technology in Spain: invasive and non-Invasive techniques for monitoring respiratory variables *Sensors* **10** 4655–74
[14] Howe T A, Jaalam K, Ahmad R, Sheng C K and Rahman N H N A 2009 The use of end-tidal capnography to monitor non-intubated patients presenting with acute exacerbation of asthma in the emergency department *J. Emerg. Med.* **41** 581–9
[15] Thompson J E and Jaffe M B 2005 Capnographic waveforms in the mechanically ventilated patient *Respir. Care* **50** 100–8
[16] Yasodananda Kumar A, Bhavani-Shankar K, Moseley H S L and Delph Y 1992 Inspiratory valve malfunction in a circle system: pitfalls in capnography *Can. J. Anaesth.* **39** 997–9
[17] Yaron M, Padyk P, Hutsinpiller M and Cairns C B 1996 Utility of the expiratory capnogram in the assessment of bronchospasm *Ann. Emerg. Med.* **28** 403–7
[18] Guthrie B D, Adler M D and Powell E C 2008 End-tidal carbon dioxide measurements in children with acute asthma *Acad. Emerg. Med.* **14** 1135–9
[19] Nagurka R *et al* 2014 Utility of initial prehospital end-tidal carbon dioxide measurements to predict poor outcomes in adult asthmatic patients *Prehosp. Emerg. Care* **18** 180–4
[20] Kassabian J, Miller K D and Lavietes M H 1982 Respiratory center output and ventilatory timing in patients with acute airway (asthma) and alveolar (pneumonia) diseases *Chest.* **81** 536–43
[21] Azab N Y, Mahalawy I I E, Aal G A A E and Taha M H 2015 Breathing pattern in asthmatic patients during exercise *Egypt. J. Chest Diseases Tuberculosis* **64** 521–7
[22] Howe T A *et al* 2011 The use of end-tidal capnography to monitor non-intubated patients presenting with acute exacerbation of asthma in the emergency department *J. Emerg. Med.* **41** 581–9
[23] Nik Hisamuddin N A R *et al* 2009 Correlations between capnographic waveforms and peak flow meter measurement in emergency department management of asthma *Int. J. Emerg. Med.* **2** 83–9
[24] Corbo J, Bijur P, Lahn M and Gallagher E J 2005 Concordance between capnography and arterial blood gas measurements of carbon dioxide in acute asthma *Ann. Emerg. Med.* **46** 323–7
[25] Balakrishnan M, Kazemi M and Howe A 2012 A review of capnography in asthma: a new approach on assessment of Capnogram (invited review) *Biotechnol. Bioinf. Bioeng.* **2** 555–66
[26] Howe T A 2001 Use of capnographic waveform indices in monitoring nonintubated asthmatic patients within the emergency department *Master Degree Thesis* Universiti Sains Malaysia
[27] Zeist Z K 1989 Mastering Infrared Capnography (Utrecht, The Netherlands: Kerckebosch-Zeist) p 101
[28] Mosenkis R 1986 Carbon dioxide monitors *Health Devices* **15** 255–85
[29] Santoso D and Setiaji F D 2013 Design and Implementation of Capnograph for Laparoscopic Surgery *Int. J. Inf. Electron. Eng.* **3** 523
[30] Moon R E and Camporesi E M 2000 Respiratory monitoring *Anaesthesia* 5th edn, ed R D Miller (New York: Churchill Livingstone) pp 1255–95
[31] Bautista C, Patel B, Shah M and Connie L 'Portable capnography' http://portablecapnography.weebly.com/uploads/8/0/5/5/8055239/nebec_portable_capnography.pdf (Accessed: 5 October 2017)
[32] binti Zaharudin S Z, Kazemi M and Malarvili M B 2014 Designing a respiratory CO2 measurement device for home monitoring of asthma severity *IEEE Conf. on Biomedical Engineering and Science* pp 230–4
[33] Gibson D and MacGregor C 2013 A novel solid state non-dispersive infrared CO2 gas sensor compatible with wireless and portable deployment *Sensors* **13** 7079–103
[34] Acker J *et al* 2013 End-tidal gas monitoring apparatus *Google Patents* (Pub. No. :WO2013003429 A1)14/129,760
[35] Zhengzhou Winsen Electronics Technology Co. 2003 *L. CO2 gas sensor module (MH410) datasheet* MH410 Winsen Technical Report http://www.isweek.com/product/ndir-infrared-co2-gas-sensor-mh-410d_143.html
[36] Julius G G 2009 Effort-independent, portable, user-operated capnograph device and related methods *Google Patents.* (Pub. No. :US20090118632 A1)12/265,574
[37] Kuhn K, Pignanelli E and Schutze A 2013 Versatile gas detection system based on combined NDIR transmission and photoacoustic absorption measurements *IEEE Sens. J.* **13** 934–40
[38] Xu S and Chen M 2012 Design and modeling of non-linear infrared transducer for measuring methane using cross-correlation method *Measurement* **45** 325–32
[39] Zhu Z, Xu Y and Jiang B 2012 A one ppm NDIR methane gas sensor with single frequency filter denoising algorithm *Sensors* **12** 12729–40

[40] Hébert L J *et al* 2011 Isometric muscle strength in youth assessed by hand-held dynamometry: a feasibility, reliability, and validity study *Pediatr. Phys. Ther.* **23** 289–99
[41] Gali F *et al* 2011 Use of maximum end-tidal CO2 values to improve end-tidal CO2 monitoring *Resp. Care.* **56** 278–83
[42] Michael Callans Reliability and Validity in Testing—What do They Mean? (cited 16 November 2016) http://blog.wonderlic.com/reliability-and-validity-in-testing-what-do-they-mean (Accessed 5 October 2017)
[43] Cramer D 1998 *Fundamental Statistics for Social Research: Step-by-Step Calculations and Computer Techniques Using SPSS for Window* (New York: Routledge)
[44] Cramer D and Laurence Howitt D 2004 *The SAGE Dictionary of Statistics: A Practical Resource for Students in the Social Sciences* 1st edn (London: SAGE Publications Ltd)
[45] Doane D P and Seward L E 2011 Measuring skewness *J. Stat. Educ.* **19** 1–18
[46] Razali N M and Wah Y B 2011 Power comparisons of shapiro-wilk, kolmogorov-simrnov, lilliefors and anderson-darling tests *J. Stat. Modelling Anal.* **2** 21–33
[47] Shapiro S S and Wilk M B 1965 *An Analysis of Variance Test for Normality (Complete Samples)* vol 52 (Oxford University Press) pp 591–611
[48] Kropmans J B *et al* 1999 Smallest detectable difference in outcome variables related to painful restriction of the temporomandibular joint *J. Dent. Res.* **78** 784–9
[49] Liaw L-J *et al* 2008 The relative and absolute reliability of two balance performance measures in chronic stroke patients *Disabil. Rehabil.* **30** 656–61
[50] Rosner B 2000 *Fundamentals of Biostatistics* 5th edn (Pacific Grove: CA: Duxbury Thomson Learning)
[51] Shrout P E and Fleiss J L 1979 Intraclass correlations: uses in assessing rater reliability *Psychol. Bull.* **86** 420–8
[52] Bland J M and Altman D 1986 Statistical methods for assessing agreement between two methods of clinical measurement *Lancet* **327** 307–10
[53] Langhan M L, Zonfrillo M R and Spiro D M 2008 Quantitative end-tidal carbon dioxide in acute exacerbation of asthma *J. Pediatr.* **152** 829–32
[54] Hockenberry M J and Wilson D 2015 *Wong's Nursing Care of Infants and Children* (Canada: Elsevier) pp 1140
[55] Yang J, An K, Wang B and Wang L 2010 New mainstream double-end carbon dioxide capnograph for human respiration *J. Biomed. Opt.* **15** 065007
[56] Kazemi M and Malarvili M B 2011 Analysis of capnogram using linear predictive coding (LPC) to differentiate asthmatic conditions *J. Tissue Sci. Eng.* **2** 1–4
[57] Thomas J R, Nelson J K and Silverman S J 2005 Research methods in physical activity *Human Kinetics* 3rd edn (Champaign, IL: Human Kinetics)
[58] Lih-Jiun L *et al* 2008 The relative and absolute reliability of two balance performance measures in chronic stroke patients *Disabil Rehabil.* **30** 656–61
[59] Brown J D 1996 *Testing in Language Programs* (Englewood Cliffs, NJ: Prentice-Hall))
[60] Brown J D (ed) 1999 *Gendo kyoiku to tesutingu, Language Teaching and Testing* (Tokyo: Taishukan Shoten) translated into Japanese by M. Wada
[61] Smiths Medical 2016 Capnography connection and patient monitoring Accessed: 16 September 2016 http://www.acphd.org/media/86883/capnography_hottopics_3_08_quiz.ppt